

THE RESEARCHES ON THE FRICTION PROPERTIES OF NC-WC/A-C COATING ON THE LIGHTWEIGHT VALVE STEM

Krzysztof Siczek

Technical University of Lodz
Department of Vehicles and Foundations of Machine Design
Zeromskiego Street 116, 90-924 Lodz, Poland
tel.: +48 42 6312250, fax: +48 42 6312252
e-mail: ks670907@p.lodz.pl

Abstract

The lightweight valves, especially made of TiAl alloys, are more and more often used in modern combustion engines with cam and camless valvetrain. To increase the wear resistance and to decrease the coefficient of friction between valve stem and valve guide, different kinds of the coating are used. The researched valve has been outlet one made of TiAl6Zr4Sn2Mo2 alloy with the original chrome coating on the valve stem. The nc-WC/a-C:H nanocoating has been deposited on the chromed stem of researched valve, which has mated with the guide made of cast iron. The aim of the present paper is to investigate friction properties of such nc-WC/a-C:H deposited onto the chromed and polished surface of the valve stem. The scheme of research stand has been presented in the paper. On the stand it has been possible to measure values of valve lift and of valve acceleration, the impact force between valve and its seat insert, the friction force between valve stem and its guide, the temperature values for valve guide and for seat insert and a sound level during impacting. Researches have been performed in conditions of room temperature and without oil lubrication in the valve stem – guide contact zone. Basing on the measured values of friction force between valve stem and its guide vs. time and loading frequency, the coefficient of friction has been estimated. Obtained curves of friction force and of friction coefficient vs. time, for different frequency values of valve loading have been presented in the article.

Keywords: nc-WC/a-C coating, TiAl alloy, lightweight valve, valvetrain, coefficient of friction

1. Introduction

For improving load-carrying capacity (higher than 1 GPa) and the tribological properties of Ti6Al4V alloy, and to decrease its proneness to seizure and dry friction coefficient against a different technical alloys, a multiplex treatment has been used, in which a gradient TiCxNy layer with superficial low friction, hydrogenated diamond-like a-C:H coating, was deposited onto an enhanced diffusion-hardened surface of a mentioned titanium alloy substrate [1]. It has been researched a series of plasma diffusion treatments of the Ti6Al4V alloy including oxidizing, nitriding and oxynitriding, with effective decrease of the wear rate, however with a friction coefficient greater than 0.3 [2]. In the review article [3], it has been given a broad spectrum of modern hard, tough and low friction, functionally graded or nanolaminate (i.e., nanostructured in one dimension) or nanocomposite coatings (i.e., nanostructured in three dimensions) on different substrates. The great tribological properties of magnetron sputtered a-C coatings have been demonstrated in [4]. The good tribological properties under dry sliding conditions of carbon-based nanocomposite coatings nc-WC/a-C and nc-WC/a-C:H has been shown in [5]. Another low friction nanocomposite nc-WC1-x/a-C coating has been researched in [6]. The nanocomposite nc-TiC/a-C and nc-TiC/a-C:H coatings deposited onto Si, AISI 304 stainless steel and high chromium X120CrW12 tool steel by means of a closed field unbalanced magnetron sputtering ion plating (CFUBMSIP) method can protect well such substrates against wear and decrease effectively the dry friction coefficient [7-9]. Hydrogenated coatings nc-CrC/a-C:H deposited by a direct-current magnetron sputtering onto Si, low alloyed carbon steel DC01 and 6-5-2 high speed (HS) steel can decrease the dry friction coefficient to a value of 0.05 [10]. Several multilayer, hybrid tribological

coatings onto Ti6Al4V alloy have been proposed in [11]. A low stress, friction reducing, gradient a-C:H(Ti) coating onto titanium alloy substrates has been researched in [12]. Several low friction and wear resistant, hydrogenated nc-MeC/a-C:H coatings as well as hydrogen-free ones have been described in [13]. A series of different nanolaminate and nanocomposite coatings has been synthesized on the surface of a diffusion-hardened Ti6Al4V alloy using a number of hybrid multiplex treatments including high density gas pulse plasma magnetron sputtering [14]. All such coatings have been of high hardness and have been of a very low roughness $\sim 0.01 \mu\text{m}$ except for the nanocomposite nc-TiN/a-SiN coating, which roughness has been much higher ($\sim 0.1 \mu\text{m}$). The coatings adherence to the surface of the diffusion hardened Ti6Al4V alloy has been very strong. It has observed that the dry friction coefficient in contact for all the coatings against 100Cr6 ball-bearing steel has decreased. Some of the coatings have decreased that coefficient even more than one order of magnitude, except for the nanocomposite nc-TiN/a-SiN coating for which no decrease of the coefficient has been obtained in comparison with clean Ti6Al4V alloy. The hydrogenated nanocomposite coatings have decreased the friction coefficient more effectively than the hydrogen-free ones.

Additionally, the value of a “strain-to-failure” ratio has been decreased with increasing fraction of the interfaces in the nanolaminate and nanocomposite coatings. Some of the coatings have decreased the wear coefficient during dry sliding to a value $2 \cdot 10^{-16} \text{ m}^3 \cdot \text{N}^{-1} \cdot \text{m}^{-1}$ close to a value characteristic for lubricated sliding couples from steels. The coatings have been highly resistant to fatigue at cyclic stress loadings of the amplitude up to 1.5 GPa [14].

The object of researches presented in the paper has been outlet valve made of TiAl6Zr4Sn2Mo2 alloy with the original chrome coating on the valve stem.

The aim of the present paper is to investigate mentioned excellent properties of nc-WC/a-C deposited onto the chromed and polished surface of the valve stem.

2. Nanocomposite nc-WC/a-C coatings deposition

The nanocomposite nc-WC/a-C coating has been deposited in a vacuum-chamber of a magnetron sputtering unit B90 described in [15] and equipped with four independent, medium frequency magnetrons placed symmetrically around a vertical axis of the chamber every 90° . For deposition of the mentioned nanocomposite coatings three of the four magnetrons were equipped with high purity (3N) graphite targets and only one with W target. Before introducing into the vacuum chamber the substrates have been washed in warm water with detergent admixture, next in acetone in an ultrasonic bath and dried with compressed nitrogen of high purity. After air evacuation, the chamber and the specimens were first heated with infrared radiators to approx. 420 K and next the specimens were submitted to glow-discharge cleaning during approx. 300 s at the negative bias potential -1 kV in a pure Ar atmosphere under a pressure of 4 Pa. After cleaning firstly a thin (approx. 50 nm thick) intermediate pure W layer was deposited during approx. 300 s at a power of 0.8 kW.

In the next step a proper nanocomposite layer has been deposited with all the four magnetrons working and at continuous rotation of the rotary table with specimens placed in the centre of symmetry of the system. The conditions of deposition of the carbon-based nanocomposite coating have been presented in Tab. 1.

Tab. 1. Deposition parameters of carbon-based nanocomposite coatings using RMS method [14]

Type of coating	Gas flow		Magnetrons power		Pressure during deposition	Bias	Time of deposition	Coating thickness
	Ar	H ₂	W target	3xC target				
	[cm ³ s ⁻¹]		[kW]		[Pa]	[V]	[s]	[μm]
nc-WC/a-C:H	24	12	0.3	4.2	0.55	50	21200	4.6

3. Coating characterization

After deposition the coatings were characterized by dynamic nanoindentation (for nanohardness and nanomodulus measurement). The results have been shown in Tab. 2. The thickness of nanocomposite coating has been equal about 0.36 μm , which value has been obtained for Ti6Al4V sample, with the same coating deposited in the same conditions (Tab. 1). The chemical compositions of the nanocomposite coatings in at.% have been very close to (14.2/85.8), as for nc-WC_{1-x}/a-C:H deposited onto Ti6Al4V sample, in the same mentioned conditions.

The results of dynamic measurements of nanohardness and nanomoduli for the nanocomposite coating deposited onto Ti6Al4V and TiAl6Zr4Sn2Mo2 alloys have been shown in Tab. 2 together with the resulting values of H/E (i.e., strain-to-failure).

Tab. 2. Nanohardness (nH) and nanomodulus (nE) for nanocomposite nc-WC/a-C deposited onto Ti6Al4V alloy [14] and onto TiAl6Zr4Sn2Mo2 (chromed) alloy

nc-WC _{1-x} /a-C:H deposited on		Ti6Al4V [19]	TiAl6Zr4Sn2Mo2 (chromed)
nH	[GPa]	17	16.6
nE	[GPa]	200	187
H/E	[-]	0.085	0.083

In particular, the dry friction coefficient of the coatings was measured against a hard steel bearing ball of 5 mm diam. under a load of 10 N, at a constant linear velocity of 0.1 ms^{-1} , at a temperature (296 \pm 2) K in static air of relative humidity (52 \pm 2) %.

4. Research stand

The researches have been made on the stand presented in the Fig. 1. It has been measured the values for impact force for valve impacting its seat insert, for friction force between valve and its guide, for displacement and acceleration of valve. Additionally the sound level has been measured by the sonometer. The temperature has been the room one. Measured values have been transmitted by control cassette into computer drive and registered there.

The scheme of the research stand for the measurement of valve lift and valve acceleration, of the impact force, of the friction force, of temperature values for valve guide and for seat insert, of sound level during impacting has been presented in the Fig. 1.

The stand has been calibrated, with the help of weights tested by the piezoelectric balance, with accuracy of 0.5 g. It has been calibrated the lines for the measurement of the friction force and of the impact force. During registration of measured voltages by A/C cart on the computer disc, the sensors of measurement lines have been loaded by weights. The results of calibration have been presented in the Fig. 2 and 3. The lines for measurement of valve lift and valve acceleration have had their characteristics determined by manufacturer. The line for valve lift has had the characteristic 2 mm/V and for the valve acceleration 0.008 V/1g respectively.

Values of friction coefficient μ have been estimated from equation (1):

$$\mu = \begin{cases} \frac{T}{R} = \frac{T}{(m_v + m_a) \cdot g \cdot \frac{h_v}{h_v - (h_G + x)}}, & \text{for case (a),} \\ \frac{T}{R_1 + R_2} = \frac{T}{(m_v + m_a) \cdot g \cdot \frac{h_g + 2(h_G + x)}{h_g}}, & \text{for case (b),} \end{cases} \quad (1)$$

where:

T - measured value of friction force between valve stem and its guide,

- R, R_1, R_2 - reaction between valve stem and its guide, depending on the case (Fig. 4),
- $g = 9.81 \text{ m/s}^2$ - gravitational acceleration,
- $x = (0 - 5) \text{ mm}$ - valve displacement,
- $m_v = 19.7 \text{ g}$ - valve mass,
- $m_a = 0.4 \text{ kg}$ - added mass,
- $h_v = 90 \text{ mm}$ - valve length,
- $h_g = 45 \text{ mm}$ - guide length,
- $h_G = 35 \text{ mm}$ - dimension between valve guide and weight centre of the valve – added mass assembly (Fig. 4).

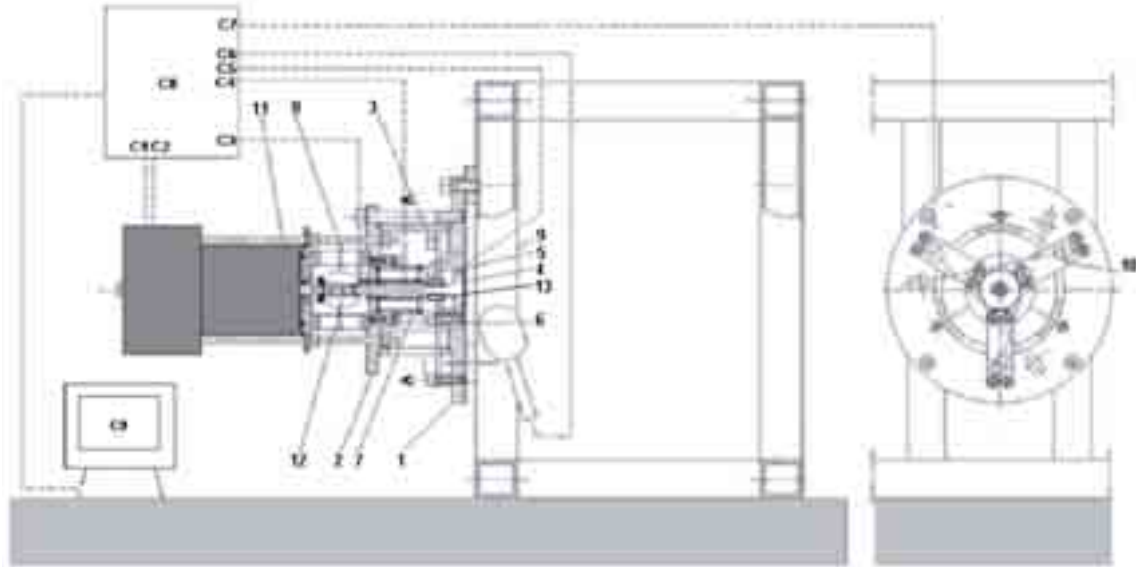


Fig. 1. The scheme of the research stand. 1 – base, 2 – cover, 3 – case sleeve, 4 – valve, 5 – seat insert, 6 – sleeve of seat insert, 7 - valve guide assembly, 8 – cantilever, 9 – frame, 10 – flat spring, 11 – driving assembly, 12 – connector, 13 – added mass, C1 – valve lift sensor, C2 – valve acceleration sensor, C3 – sensor of friction force between valve and valve guide, C4 – valve guide temperature sensor, C5 – seat insert temperature sensor, C6 – sound level meter, C7 – impact force sensor for valve impacting seat insert, C8 – control cassette, C9 – computer

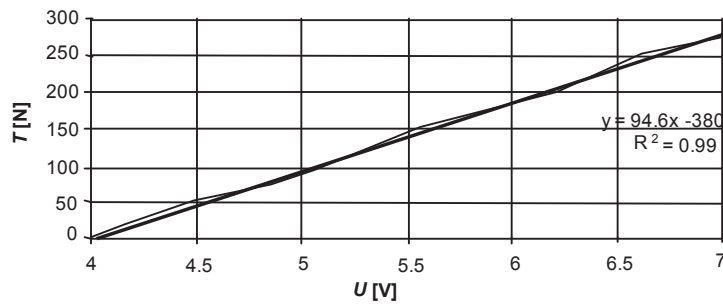


Fig. 2. The dependency of friction force T on the registered voltage U , for valve stem mating valve guide

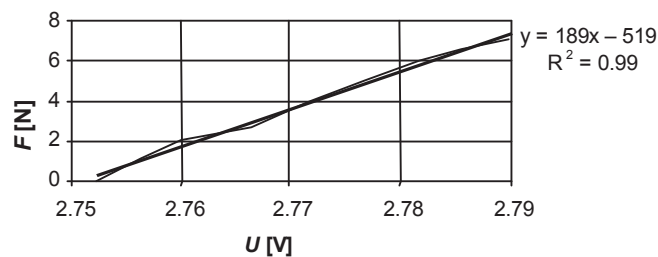


Fig. 3. The dependency of the impact force F on the registered voltage U , for the valve impacting its seat inserts

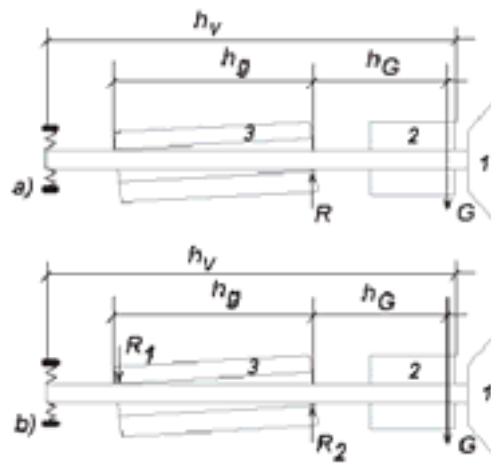


Fig. 4. The scheme of loading for the valve – added mass – guide assembly; 1 – valve, 2 – added mass, 3 – valve guide, $G = (mv+ma) \cdot g$ – loading force; a) loading case, when reaction R between valve stem and its guide has existed in only one place, b) loading case, when reactions R_1 and R_2 between valve stem and its guide have existed in two places

5. Research results

Obtained results of researches have been presented in the Fig. 4-7. Measured values of valve displacement vs. time have been shown in the Fig. 4. Valve lift has been equal 5 mm. Observed changes of valve position, during valve contact with its seat insert have resulted from the stiffness of the measuring set. Measured values of valve acceleration vs. time have been shown in the Fig. 5. The maximum value has been obtained during valve impact into its seat insert. Measured values of impact force between valve and its seat insert vs. time have been presented in the Fig. 6. After the impact, the valve have been pushed into its seat insert by the force, which value has been equal 50 N. Measured values of friction force have been presented in the Fig. 7. Values, pointed T_{max} , obtained during rising and setting of valve have been slightly different. Observed changes in friction force values have been resulted from the stiffness of the measuring set.

Values of friction coefficient, calculated from equation (1) vs. time have been presented in the Fig. 8. They have been obtained for loading frequency $f = 16$ Hz, and maximal valve lift $h_{max} = 5$ mm and they have been equal from 0.135 to 0.23. Such values vs. loading frequency have been shown in the Fig. 9. They have decreased with frequency increasing, almost linearly.

In the Fig. 10, the minimum μ_{min} and maximum μ_{max} calculated values for coefficient of friction, obtained from measured maximum friction force T_{max} between valve stem and its guide (Fig. 7) have been compared with values of dry friction coefficient of a steel bearing-ball against Ti6Al4V [14] measured against friction path Δl ; for different surfaces. It has been noted that values of dry friction coefficient for nc-WC/a-C:H coating had been close to minimum values for friction coefficient between valve stem and its guide.

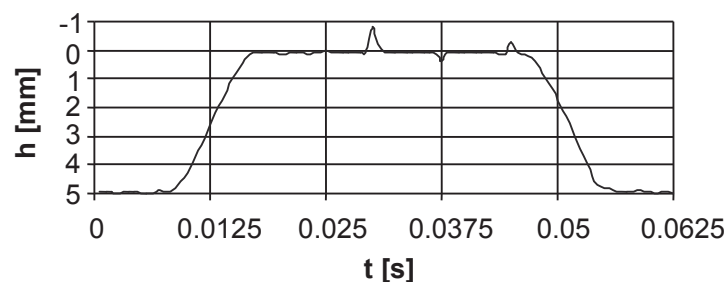


Fig. 4. Measured valve displacement h vs. time t : loading frequency $f = 16$ Hz, maximum valve lift $h_{max} = 5$ mm

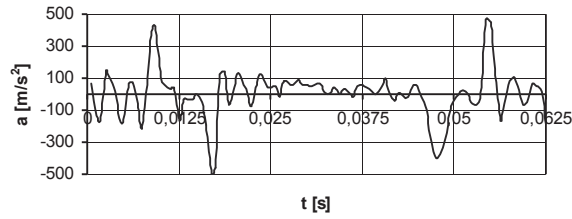


Fig. 5. Measured valve acceleration a vs. time t : loading frequency $f = 16$ Hz, maximum valve lift $h_{max} = 5$ mm

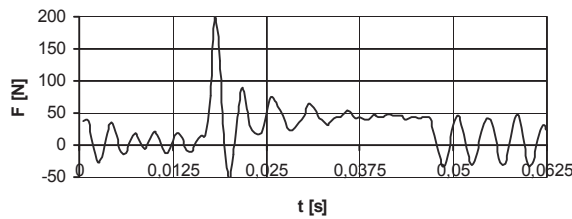


Fig. 6. Measured impact force F between valve and its seat insert vs. time t : loading frequency $f = 16$ Hz, maximum valve lift $h_{max} = 5$ mm

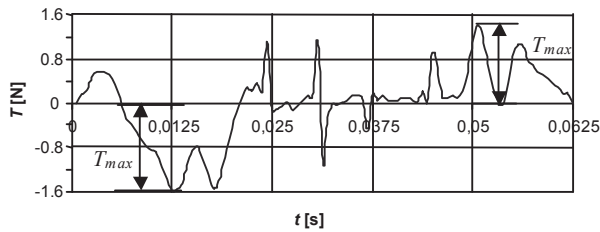


Fig. 7. Measured values of friction force T between valve and its guide vs. time t : loading frequency $f = 16$ Hz, maximum valve lift $h_{max} = 5$ mm, T_{max} – maximum friction force during valve displacement against its guide

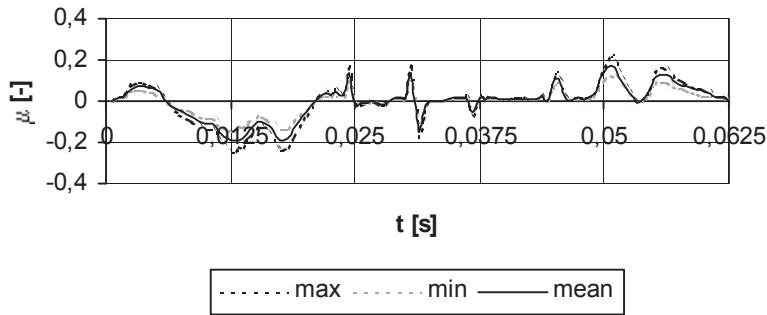


Fig. 8. Calculated values of friction coefficient μ between valve and its guide vs. time t : loading frequency $f = 16$ Hz, maximum valve lift $h_{max} = 5$ mm

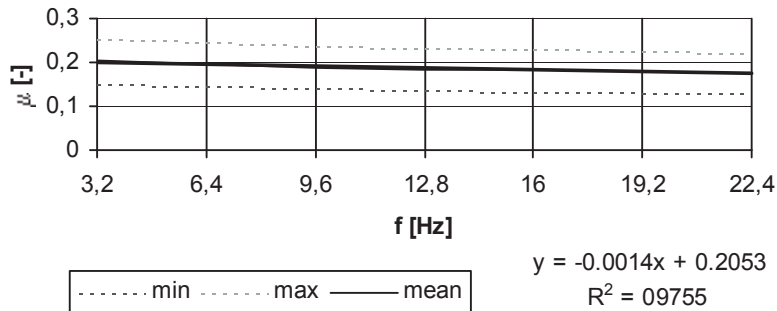


Fig. 9. Calculated values of friction coefficient μ between valve and its guide vs. loading frequency f ; maximum valve lift $h_{max} = 5$ mm

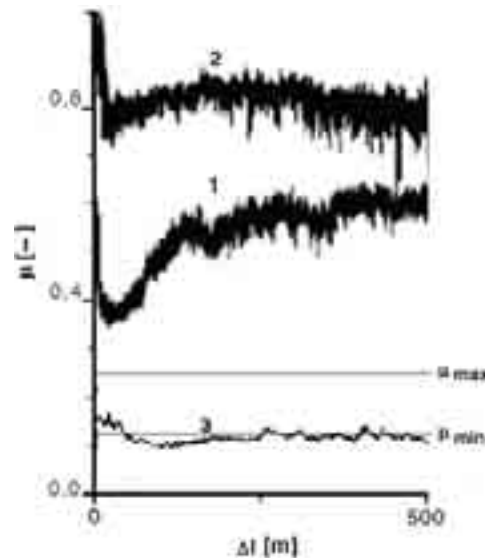


Fig. 10. Dry friction coefficient of a steel bearing-ball against Ti6Al4V μ [14] vs. friction path Δl ; μ_{min} , μ_{max} – minimum and maximum calculated value for coefficient of friction obtained from measured maximum friction force T_{max} between valve stem and its guide (Fig. 7; (a): 1 - substrate as delivered; 2 - diffusion hardened; 3 - nc-WC/a-C:H

In all cases the measured sound level have been equal 95 dBA, when sound level of laboratory environment has been equal 40 dBA

6. Conclusions

1. Values of dry friction coefficient for nc-WC/a-C:H coating have been close to minimum values for friction coefficient between valve stem and its guide.
2. Calculated values for coefficient of friction between valve stem and its guide can change from 0.13 to 0.23, depending on the reactions set (Fig. 4).
3. Friction coefficient values have decreased almost linearly with loading frequency increasing.

References

- [1] Wendler, B. G., Pawlak, W., *Low friction and wear resistant coating systems on Ti6Al4V alloy*, Journal of Achievements in Materials and Manufacturing Engineering 26/2, 207-210, 2008.
- [2] Yetim, A. F., Yildiz, F., Vangolu, Y., Alsaran, A., Celik, A., *Several plasma diffusion processes for improving wear properties of Ti6Al4V alloy*, Wear, Vol. 267, pp. 2179-2185, 2009.
- [3] Voevodin, A. A., Zabinski, J. S., Muratore, C., *Recent Advances in Hard, Tough, and Low Friction Nanocomposite Coatings*, Tsinghua Science and Technology, Vol. 10/6, pp. 665-679, 2005.
- [4] Yang, S., Camino, D., Jones, A. H. S., Teer, D. G., *Deposition and tribological behaviour of sputtered carbon hard coatings*, Surface and Coatings Technology, Vol. 124, pp. 110-116, 2000.
- [5] Czyzniewski, A., *Deposition and some properties of nanocrystalline WC and nanocomposite WC/a-C:H coatings*, Thin Solid Films, Vol. 433, pp. 180-185, 2003.
- [6] Wendler, B. G., Nolbrzak, P., Pawlak, W., Rylski, A., *Structure and properties of WC1-x/C coatings deposited by reactive magnetron sputtering on ASP2023 HSS steel and monocrystalline Si substrates*, Materials Engineering, Vol. 165-166/5-6, pp. 655-657, 2008.

- [7] Zehnder, T., Patscheider, J., *Nanocomposite TiC/a-C:H hard coatings deposited by reactive PVD*, Surface and Coatings Technology, Vol. 133-134, pp. 138-144, 2000.
- [8] Pei, Y. T., Galvan, D., De Hosson, J. Th. M., Strondl, C., *Advanced TiC/a-C:H nanocomposite coatings deposited by magnetron sputtering*, Journal of the European Ceramic Society, Vol. 26, pp. 565–570, 2006.
- [9] Lin, J., Moore, J. J., Mishra, B., Pinkas, M., Sproul, W. D., *Syntheses and characterization of TiC/a:C composite coatings using pulsed closed field unbalanced magnetron sputtering (P-CFUBMS)*, Thin Solid Films, Vol. 517, pp. 1131-1135, 2008.
- [10] Gassner, G., Mayrhofer, P. H., Patscheider, J., Mitterer, C., *Thermal stability of nanocomposite CrC/a-C:H thin films*, Thin Solid Films, Vol. 515, pp. 5411-5417, 2007.
- [11] Pawlak, W., Wendler, B., *Multilayer, hybrid PVD coatings on Ti6Al4V titanium alloy*, Journal of Achievements in Materials and Manufacturing Engineering, Vol. 37/2, pp. 660-667, 2009.
- [12] Batory, D., Stanishevsky, A., Kaczorowski, W., *The effect of deposition parameters on the properties of gradient a-C:H/Ti layers*, Journal of Achievements in Materials and Manufacturing Engineering, Vol. 37/2, pp. 381-386, 2009.
- [13] Włodarczyk, K., Makówka, M., Nolbrzak, P., Wendler, B., *Low friction and wear resistant nanocomposite nc-MeC/a-C and nc-MeC/a-C:H coatings*, Journal of Achievements in Materials and Manufacturing Engineering 37/2, pp. 364-360, 2009.
- [14] Wendler, B., Moskalewicz, T., Progalskiy, I., Pawlak, W., Makówka, M., Włodarczyk, K., Nolbrzak, P., Czyska-Filemonowicz, A., Rylski, A., *Hard and superhard nanolaminate and nanocomposite coatings for machine elements based on Ti6Al4V alloy*, Journal of Achievements in Materials and Manufacturing Engineering, Vol. 43, Is. 1, 2010.
- [15] Wendler, B. G., Danielewski, M., Przybylski, K., Rylski, A., Kaczmarek, S., Jachowicz, M., *New type AlMo-, AlTi- or Si-based magnetron sputtered protective coatings on metallic substrates*, Journal of Materials Processing Technology, Vol. 175, pp. 427-432, 2006.